PROCEEDINGS OF SCIENCE

Detection of sub-100 GeV γ-ray pulsations from PSR B1706−44 with H.E.S.S.

M. Spir-Jacob[∗1], **A. Djannati-Ataï**[1], **L. Mohrmann**[2], **G. Giavitto**[3], **B. Khelifi**[1], **B. Rudak**[4], **C. Venter**[5], **R. Zanin**[6] **for the H.E.S.S. Collaboration**[7]

[1] *APC, Université de Paris, CNRS/IN2P3, CEA/Irfu, Observatoire de Paris, 75205 Paris, France*

[2] *Friedrich-Alexander-Universität Erlangen-Nürnberg, Erlangen Centre for Astroparticle Physics, Erwin-Rommel-Str. 1, D 91058 Erlangen, Germany*

[3] *DESY, D-15738 Zeuthen, Germany*

[4] *Nicolaus Copernicus Astronomical Center, Polish Academy of Sciences, ul. Bartycka 18, 00-716 Warsaw, Poland*

[5] *Centre for Space Research, North-West University, Potchefstroom 2520, South Africa*

[6] *Max-Planck-Institut für Kernphysik, P.O. Box 103980, D 69029 Heidelberg, Germany*

[7] *for collaboration list see PoS(ICRC2019)1177*

We report on the detection of pulsations from PSR B1706−44 based on 28.3 hours of observations with the H.E.S.S. II array with CT5 in monoscopic mode. The lightcurve is similar to that obtained with the *Fermi*-LAT above 15 GeV and the pulsations exhibit a steep spectrum with index ~ -3.8 in the sub 20 GeV to sub-100 GeV energy range. While a significant signal of ~ 1000 events is detected at energies ~ 70 GeV, it is not possible to either confirm or rule out a power-law behaviour of PSR B1706−44 spectrum in this range.

36th International Cosmic Ray Conference -ICRC2019-
July 24th - August 1st, 2019
Madison, WI, U.S.A.

∗Speaker.

http://pos.sissa.it/

1. Introduction

The 28 m equivalent diameter telescope (CT5), added in 2012 to the core of the H.E.S.S. array of four 12 m diameter imaging atmospheric Cherenkov telescopes (CT1-4) has allowed to reach sub-20 GeV energies in monoscopic mode for observations of pulsars [8, 13], thus bridging the gap to satellite-based γ-ray instruments.

After the Vela and Crab pulsars, which have both been detected from ground [13, 26, 6, 7], PSR B1706−44 is the third brightest γ-ray-ray emitting pulsar [2]. Its spin-down power of $\dot{E} = 3.4 \times 10^{36}$ erg/s and age, $\sim 1.7 \times 10^4$ years are very similar to those of the Vela pulsar. Despite its rather large distance of ∼2.3 kpc as compared to Vela (294 pc), the γ-ray-ray luminosity of PSR B1706−44 at 10 GeV is only 3 times lower than Vela, and as such, it constituted a promising target for detection from ground.

γ-rays were first detected from PSR B1706−44 with the COS-B satellite in 1981 [24], classified as an unidentified source. It was only identified a decade later as a 102 ms pulsar with the Parkes radio telescope [16]. PSR B1706−44 has since been detected with EGRET [25], *Chandra* [12], AGILE [21] and *Fermi*-LAT [1]. The synchrotron nebula around PSR B1706−44 [10] displays a surprisingly low radio flux in comparison with other radio pulsar wind nebulae (PWNe) [11], and in X-rays, *ROSAT* and *ASCA* have revealed a structure of a torus and a jet [9]. In VHE γ-rays, an extended source of Gaussian width 0.29° was discovered by H.E.S.S. above 600 GeV [14], of which the association with PSR B1706−44 is likely but not firmly established.

2. Observations and data analysis

2.1 H.E.S.S.

H.E.S.S. observations were carried out during two campaigns in 2013 and 2015. They were made in wobble mode with an offset range of $0.2° - 0.7°$, and an average zenith angle of 24.5°. After quality selection for smooth telescope operation and good weather conditions, 28.3 hours of data out of the 38 hours of observations were kept.

The monoscopic analysis pipeline used for this detection is the same as the one originally developed and validated on Vela pulsar data with CT5 [13]. It was used to reconstruct the shower direction, impact and energy of the primary γ-rays, based on the recorded shower images. The images were obtained after calibration and image cleaning. To compute the phase of each event, the time stamps provided by the central trigger system of H.E.S.S. were folded using the `Tempo2` package [15] with an ephemeris derived from radio data from the Parkes Radio Telescope [22], valid between 22$^{\text{nd}}$ of July 2007 till 11$^{\text{th}}$ of September 2015. To discriminate between photons and hadrons, a boosted decision tree (BDT), trained on γ-ray Monte Carlo (MC) simulations for the signal and on real data for the background, was used. Background was additionally rejected through a spatial cut at a 68%-containment radius (0.3°) and by a selection in phase. For the latter, ON- and OFF-phase ranges were defined based on the *Fermi*-LAT phasogram (see below) and a maximum likelihood-ratio test [17] was applied to compute the significance of the signal.

The energy spectrum for H.E.S.S. data was derived using a maximum likelihood fit within a forward-folding scheme [20]. The instrument response functions (IRFs) were computed through extensive MC simulations as a function of the energy, zenith, and azimuthal angles of the telescope pointing direction, the impact parameter of showers, and the configuration of the telescope for each observing period.

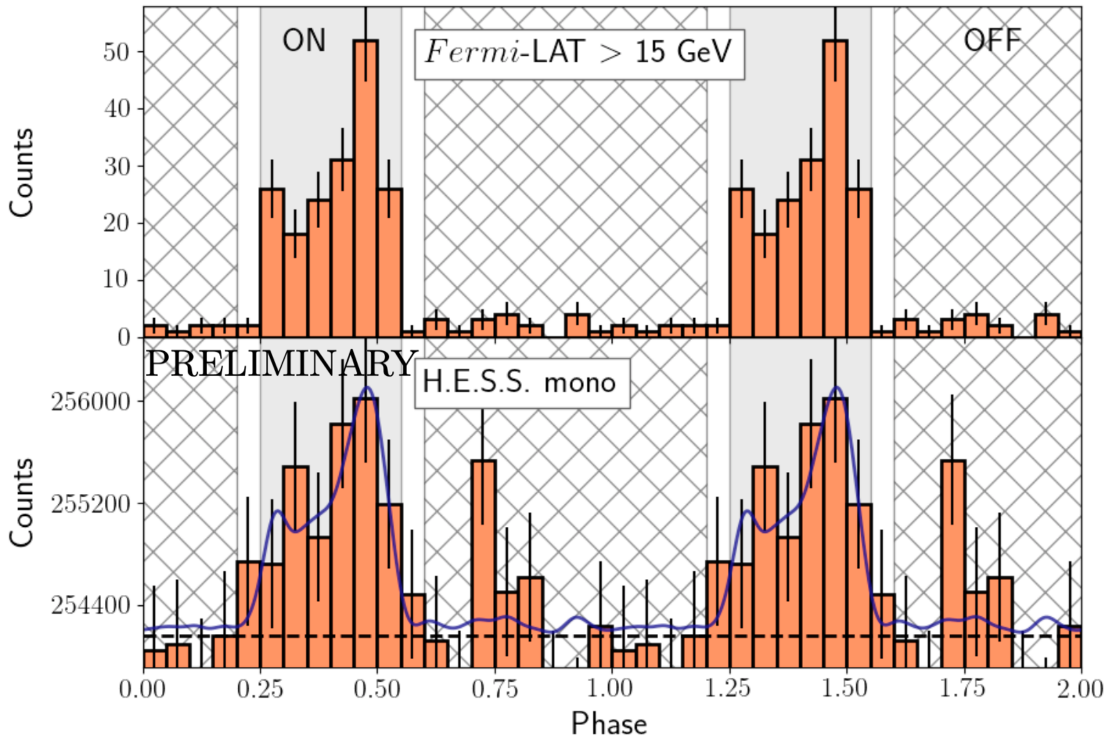

Figure 1: Histogram of phases for two periods with *Fermi*-LAT data > 15 GeV (top) and H.E.S.S. II with CT5 in monoscopic mode data (bottom). The hashed box represents the OFF-pulse region and the grey box the ON-pulse region. The dashed line shows the average level of background evaluated in the OFF-pulse region. From the *Fermi*-LAT data above 15 GeV, we derive a KDE (variance of 0.025), represented by the blue curve and used for a maximum-likelihood ratio test on the H.E.S.S. II-CT5 data.

2.2 *Fermi*-LAT

62 months of *Fermi* data from 2008 to 2013 were used to derive the phasogram and phased-resolved spectra above two energy thresholds of 100 MeV and 10 GeV.

Events were selected from the P8 Source class (event class = 128, event type =3) within a region of interest (ROI) of 10° radius around the position of the pulsar, and `P8R2_SOURCE_V6` IRFs were used. Only γ-ray events with reconstructed zenith angles smaller than 90° were selected in order to reduce contamination by γ-rays from Earth's limb.

The pulsar phase was computed for selected events using the `Tempo2` *Fermi* plug-in [23] and the same ephemeris as that used for the H.E.S.S. data.

An additional selection cut $\theta_{\max} = 0.6°$ was applied on the angular distance of each photon to the pulsar position for generation of the light curves. This cut value is slightly smaller than the 68% and 95% containment radii of the *Fermi*-LAT at 1 and 10 GeV, respectively, and allows us to retain a large number of highest energy photons, while limiting the background in the $1-10$ GeV range.

The spectral analysis was done using `gtlike` tool, the Galactic diffuse emission model, `gll_iem_v06.fits`, and isotropic diffuse model, `iso_P8R2_SOURCE_V6_v06.txt`. All sources from the *Fermi*-LAT third source catalogue (3FGL) [5], within a region of 20° radius centred on the pulsar position were added to the source model, while parameters for sources outside the ROI were fixed during the fit.

3. Results

3.1 Light Curves

Figure 1 shows the phasogram of PSR B1706−44 for the *Fermi*-LAT data above 15 GeV (on top) and for the H.E.S.S. data (on the bottom). Two periods are displayed for better readability. The light curve of PSR B1706−44 at lower energies, e.g. 1 GeV, consists of two peaks spanning in the [0.25-0.55] phase range and connected with a large-amplitude bridge [3]. The [0.25-0.55] and [0.6-0.2] intervals were subsequently defined as the ON- and OFF-phase ranges, respectively.

The H.E.S.S. II-CT5 light curve contains 5 091 420 events, with 1 532 177 in the ON-phase and 3 050 011 in the OFF-phase, which corresponds to a 7171.5± 1515 excess. The source is detected at a significance level of 4.74σ (Li&Ma test [18]). An alternative pipeline ([19]) was used as a cross-check and validated the detection, at a slightly lower significance. We note that the phase bins near phase 0.75 exhibit some excess but at a low significance level when taking into account the trials. The probability density function (PDF) of the *Fermi*-LAT light curve is derived through a KDE (with variance 0.025), and used in a maximum-likelihood ratio test on the H.E.S.S. data. The test significance value of 4.6σ and excess number of 8139 events are compatible with those obtained with the Li & Ma test. The larger number of excess can be due to the contribution of some events near phase 0.75.

3.2 Spectra

The spectra obtained with both instruments and with the phase definitions given above are shown in Fig. 2. For the *Fermi*-LAT data, phase-resolved spectra were derived first above 100 MeV, assuming a power law with an exponential cut-off (ECPL):

$$\mathrm{d}N(E)/\mathrm{d}E = N_0\,(E/E_0)^{-\Gamma}\exp\left[-(E/E_\mathrm{c})^b\right].$$

The best-fit values obtained are $N_0 = (1.05 \pm 0.05^{\mathrm{stat}}) \times 10^{-9}$ MeV^{-1}cm^{-2}s^{-1}, $\Gamma = 1.19 \pm 0.01$, $b = 0.48 \pm 0.01$ and $E_c = 403 \pm 10$ MeV at a reference energy of 1 GeV. The fit of a power law above 10 GeV yielded in turn an index $\Gamma_{\mathrm{LAT}} = 3.9 \pm 0.1$ and a flux normalisation at the reference energy of 20 GeV $N_0 = (4.4 \pm 0.3^{\mathrm{stat}}) \times 10^{-8}$ MeV^{-1}cm^{-2}s^{-1}. The fit of a parabola model (LPB, $\mathrm{d}N(E)/\mathrm{d}E = \Phi_0\,(E/E_0)^{-\Gamma_{\mathrm{LPB}}-\beta\;\ln(E/E_0)}$) was performed to investigate curvature above 10 GeV, and resulted in $\Gamma_{\mathrm{LPB}} = 4.1 \pm 0.2$ and $\beta = 0.5 \pm 0.4$. The likelihood ratio between the parabola model and the power law yields a significance of only 1.4σ in favor of the curvature. This, however, does not preclude the exponential cut-off found with the larger energy range fit, although one might be in the same situation as that of the Crab, i.e. an apparent curvature due to lack of statistics.

For the H.E.S.S. II-CT5 data, a power-law fit resulted in an index $\Gamma_{\mathrm{HESS}} = 3.76 \pm 0.36^{\mathrm{stat}}$, a normalization $\Phi_0^{\mathrm{HESS}} = (4.3 \pm 0.9^{\mathrm{stat}}) \times 10^{-8}$ TeV^{-1}cm^{-2}s^{-1}, at the reference energy $E_0 = 20$ GeV, and with decorrelation energy $E_\mathrm{d} = 21.5$ GeV. It was shown in [13] that the threshold of CT5 is

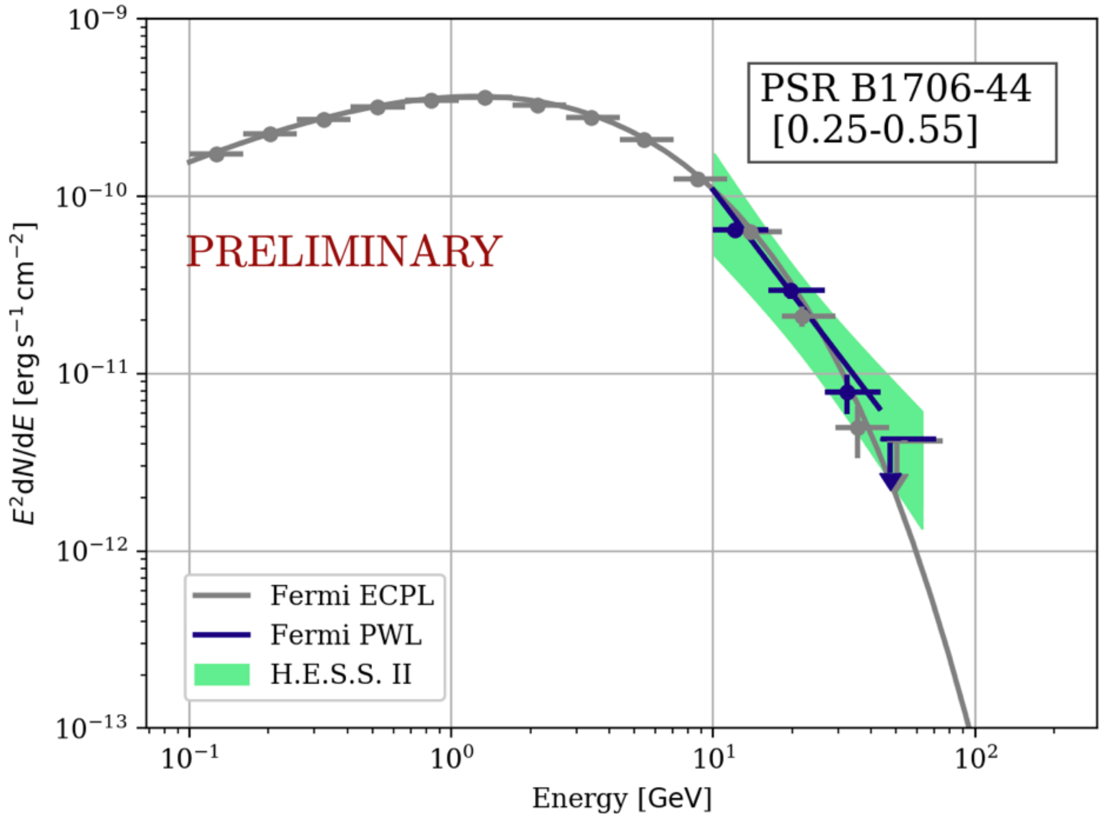

Figure 2: PSR B1706-44 spectral energy distribution. The grey and blue flux points are obtained from 5 years of *Fermi* data. Two fits are plotted: the power law with a sub-exponential cutoff above 100 MeV (grey) and another power law for the tail of the emission above 10 GeV (blue). The green box is derived from 28.3 hours of H.E.S.S. II-CT5 data and includes systematic errors (see text).

close to 10 GeV. Here, again, the CT5 data fit results are in full agreement with the ones obtained from the LAT above 10 GeV.

The fit of a parabola model was not attempted due to lack of statistics and rather low signal-to-noise ratio. The higest energy bin in the CT5 data lies in the range [54-225] GeV displays an excess of 2782 events at a significance level of 2.5σ. Due to the large bias in energy reconstruction (see [13]), the average energy in this bin differs from a simple weighted mean taking into account the spectral index. An evaluation using a simulated spectrum with parameters matching those of the *Fermi*-LAT power law above 10 GeV predicts that 60% of events with $< E >$=62.7 GeV and with a dispersion of 37 GeV lie in that bin. The confidence box of the H.E.S.S. SED, shown in Fig 2 is hence limited to 62.7 GeV. The box includes the systematic errors obtained with the procedure described in [13], except that the energy scale uncertainty used here is +5% instead of +8%. The latter value was an upper limit for the relative energy scale offset between *Fermi*-LAT and H.E.S.S. II-CT5. The correction to +5% is due to the LAT recalibration on electrons [4] which brought the LAT scale 3% down in energy, i.e. closer to CT5 scale.

4. Summary

A significant pulsed signal from PSR B1706−44 has been detected with 28.3 hours of observations with H.E.S.S. II-CT5 in monoscopic mode. This is the fourth detection of a pulsar from the ground, after the Crab, Vela and Geminga pulsars.

The phasogram obtained with H.E.S.S. II-CT5 is similar to that of *Fermi*-LAT above 15 GeV, i.e. the peak P2 is clearly dominant over P1, in continuity with the trend seen at lower energies [3]. The comparison of the CT5 spectrum with that obtained from 5 years of *Fermi*-LAT data above 10 GeV shows a very good agreement. The pulsed spectrum of PSR B1706−44 above 10 GeV is shown to be very steep (index~ -3.8 to 3.9) with both *Fermi*-LAT and H.E.S.S. II-CT5 and similar to the Vela puslar [13]. However, the lack of statistics in either instrument data prevents any conclusion on the absence or presence of a spectral curvature/cut-off. The question hence remains whether PSR B1706-44's spectrum behaves like the Vela PSR where an indication of curvature at a level $> 3\sigma$ was found independently with both *Fermi* and H.E.S.S. II-CT5 [13], or as the Crab pulsar where a soft and tail-like extension of the *Fermi*-LAT spectrum was found above 100 GeV and extending up to 1 TeV [26, 6, 7]. Measuring the behaviour of the tail of the spectrum in the tens of GeV range should bring further insights into mechanisms at play in young pulsars, including those in the VHE regime. This would require further observations with H.E.S.S. or CTA.

5. Acknowledgements

See: `https://www.mpi-hd.mpg.de/hfm/HESS/pages/publications/auxiliary/HESS-Acknowledgements-2019.html`

References

[1] Abdo, A. A., Ackermann, M., Ajello, M., et al. 2010, ApJS, 187, 460

[2] Abdo, A. A., Ajello, M., Allafort, A., et al. 2013, ApJS, 208, 17

[3] Abdo, A. A., Ajello, M., Antolini, E., et al. 2010, ApJ, 720, 26

[4] Abdollahi, S., Ackermann, M., Ajello, M., et al. 2017, Phys. Rev. D, 95, 082007

[5] Acero, F., Ackermann, M., Ajello, M., et al. 2015, ApJS, 218, 23

[6] Aleksić, J., Alvarez, E. A., Antonelli, L. A., et al. 2011, ApJ, 742, 43

[7] Ansoldi, S., Antonelli, L. A., Antoranz, P., et al. 2016, A&A, 585, A133

[8] Djannati-Ataï, A., Giavitto, G., Holler, M., et al. 2017, in American Institute of Physics Conference Series, Vol. 1792, 6th International Symposium on High Energy Gamma-Ray Astronomy, 040028

[9] Finley, J. P., Srinivasan, R., Saito, Y., et al. 1998, ApJ, 493, 884

[10] Frail, D. A., Goss, W. M., & Whiteoak, J. B. Z. 1994, ApJ, 437, 781

[11] Giacani, E. B., Frail, D. A., Goss, W. M., & Vieytes, M. 2001, AJ, 121, 3133

[12] Gotthelf, E. V., Halpern, J. P., & Dodson, R. 2002, ApJ, 567, L125

[13] H. E. S. S. Collaboration, Abdalla, H., Aharonian, F., et al. 2018, A&A, 620, A66

[14] H. E. S. S. Collaboration, Abramowski, A., Acero, F., et al. 2011, A&A, 528, A143

[15] Hobbs, G. B., Edwards, R. T., & Manchester, R. N. 2006, MNRAS, 369, 655

[16] Johnston, S., Lyne, A. G., Manchester, R. N., et al. 1992, MNRAS, 255, 401

[17] Li, T.-P. & Ma, Y.-Q. 1983, ApJ, 272, 317

[18] Li, T. P. & Ma, Y. Q. 1983, ApJ, 272, 317

[19] Murach, T., Gadjus, M., & Parsons, R. 2015, in Proc. 34th Intern. Cosmic Ray Conf. No. 1022

[20] Piron, F., Djannati-Atai, A., Punch, M., et al. 2001, A&A, 374, 895

[21] Pittori, C., Verrecchia, F., Chen, A. W., et al. 2009, A&A, 506, 1563

[22] Ray, P. S., Kerr, M., Parent, D., et al. 2011, The Astrophysical Journal Supplement Series, 194, 17

[23] Ray, P. S., Kerr, M., Parent, D., et al. 2011, ApJS, 194, 17

[24] Swanenburg, B. N., Bennett, K., Bignami, G. F., et al. 1981, ApJ, 243, L69

[25] Thompson, D. J., Arzoumanian, Z., Bertsch, D. L., et al. 1993, Nature, 365, 188

[26] VERITAS Collaboration, Aliu, E., Arlen, T., et al. 2011, Science, 334, 69

PoS(ICRC2019)799